Hoek, E and Guevara, R. 2009. **Overcoming squeezing in the Yacambú-Quibor tunnel, Venezuela**. *Rock Mechanics and Rock Engineering*, Vol. 42, No. 2, 389 - 418.

Overcoming squeezing in the Yacambú-Quibor tunnel, Venezuela

by

Evert Hoek
Consulting Engineer, Vancouver, Canada
Corresponding Author: ehoek@mailas.com

Rafael Guevara Briceño
Consulting Engineer, Caracas, Venezuela

Abstract

The 5 m diameter 23.3 km long Yacambú-Quibor tunnel is designed to carry water through the Andes from the Yacambú dam in the wet tropical Orinoco basin to the semi-arid but fertile Quibor basin in western Venezuela. The tunnel is excavated in silicified and graphitic phyllites at depths of up to 1270 m below surface and extreme squeezing problems have been encountered. Construction involved 8 contracts extending over 32 years with breakthrough being achieved in July 2008. Several excavation methods and various lining designs were used over the years until the adoption of yielding support permitted the Owner and the Contractor to agree that only a circular section would be used and emphasis was placed on developing a routine construction procedure, irrespective of the rock conditions encountered at the face. This paper describes some of the rock engineering issues that were faced during the construction of this tunnel.

Keywords

Tunnel lining, squeezing, yielding support, support capacity calculation, graphitic phyllite, steel sets, sliding joints, shotcrete lining

Overcoming squeezing in the Yacambú-Quibor tunnel, Venezuela

Evert Hoek and Rafael Guevara

Introduction

The Yacambú-Quibor tunnel in the State of Lara in Venezuela finally broke through on 27 July 2008 after 32 years of technical, financial, contractual and political problems. The 4.0 m average internal diameter 23.3 kilometre long tunnel will transfer 347 million cubic metres water per year from the wet tropical Orinoco basin, on the eastern flank of the Andes, to semi arid Quibor valley on the western flank of the Andes. The agricultural and urban requirements of this semi-arid agricultural area, near the city of Barquisimeto, exceed currently available fresh water supplies and have resulted in a significant depletion of aquifers in the Quibor region.

The principal technical issues that had to be overcome were the severe squeezing problems in very weak graphitic phyllites at depths of up to 1270 m below surface. Initial attempts to use an open-face TBM in 1976 failed as did attempts to use heavy support to resist squeezing. It was only after the introduction of yielding support in about 1991 that reasonable progress was made. Difficulties continued with floor heave in sections of the tunnel in which horseshoe profiles were used, even after the introduction of yielding support. Finally, in 2004, slow but steady progress was achieved after the Owner and the Contractor agreed that only a circular section would be used and emphasis was placed on developing a routine construction procedure, irrespective of the rock conditions encountered at the face.

Project background

The location of the project, near the city of Barquisimeto, is shown in Figure 1. A plan of the tunnel alignment is shown in the inset figure. A vertical cross-section along the tunnel alignment is given in Figure 2. The location of the Bocono Fault, which is 750 m wide at tunnel elevation, is shown in this figure.

The north-western region of South America and Panama is one of the most tectonically complex land regions on earth as illustrated in Figure 3. Four major plates interact in the region. The Andes follow the north-south Nazca/South American plate boundary to the south but curve eastward in the north and they are influenced by this complex tectonic junction. In particular, in the region of Yacambú-Quibor project (circle in the upper right of the figure) a triangle of strike-slip and transpressional faults (including the Bocono) react to accommodate the mismatch in movement of the surrounding plates. The phyllitic rock mass which dominates the mountain range in the Yacambú-Quibor area ranges from strong and reasonably massive silicified phyllites in the dam area to severely tectonically deformed graphitic phyllite along most of the tunnel alignment.

The original site investigations, dating back to the 1970s, involved walk-over surveys, core drilling and the construction of several exploration adits. Most of the drilling and the adits were concentrated in the silicified phyllite in the area of the Yacambú dam site where some of the exploration tunnels have stood, without any support, for more than 40 years. The strength of the silicified phyllite is exemplified in the steep sided canyon in which the 160 m high concrete faced rockfill dam is located and by the steep downstream face of this ridge, shown in Figure 4.

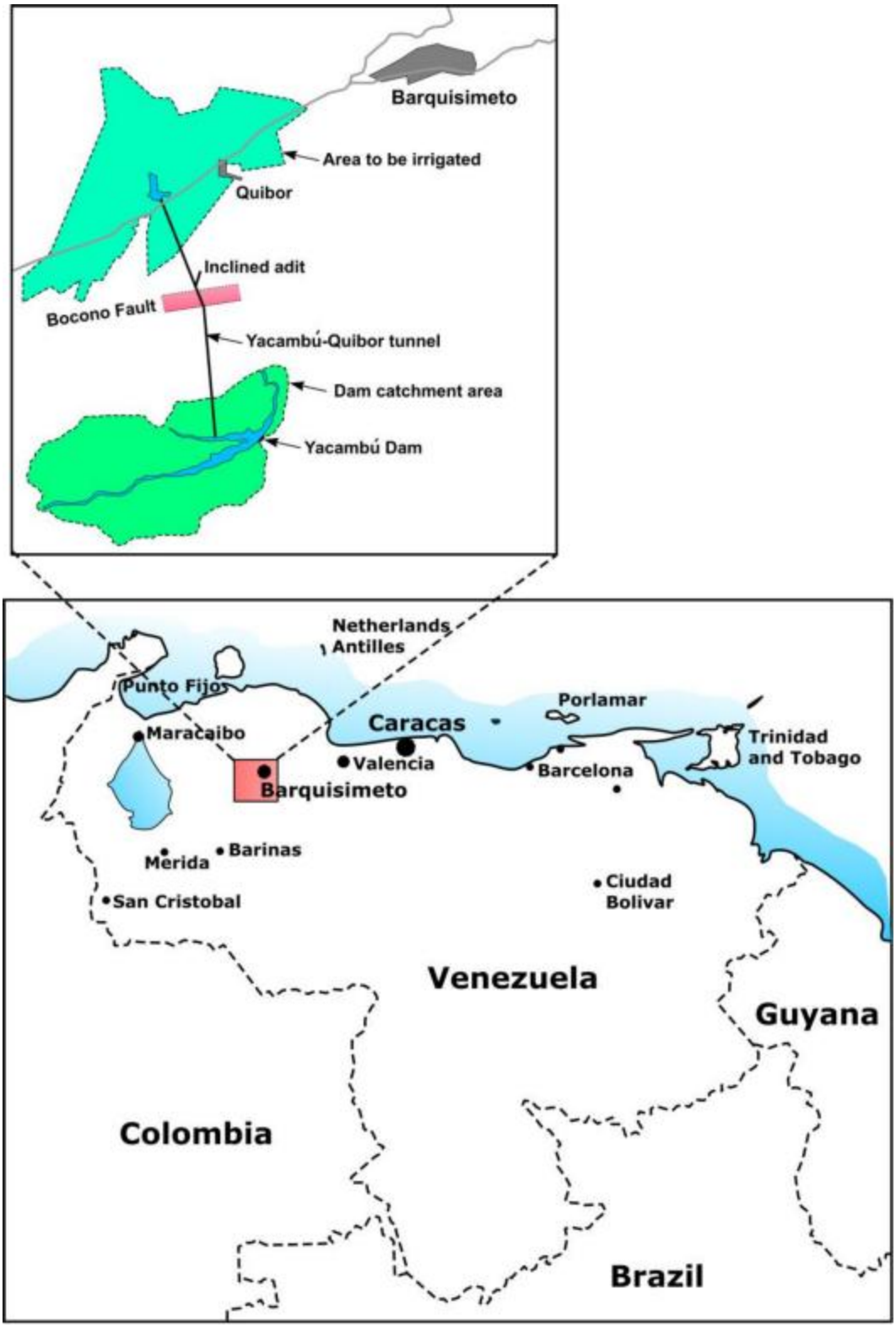

Figure 1: Project location.

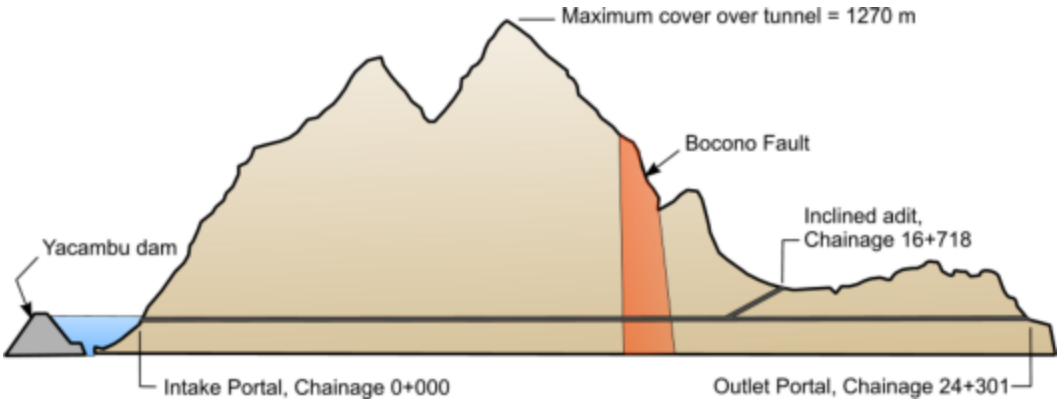

Figure 2: Cross-section along tunnel alignment.

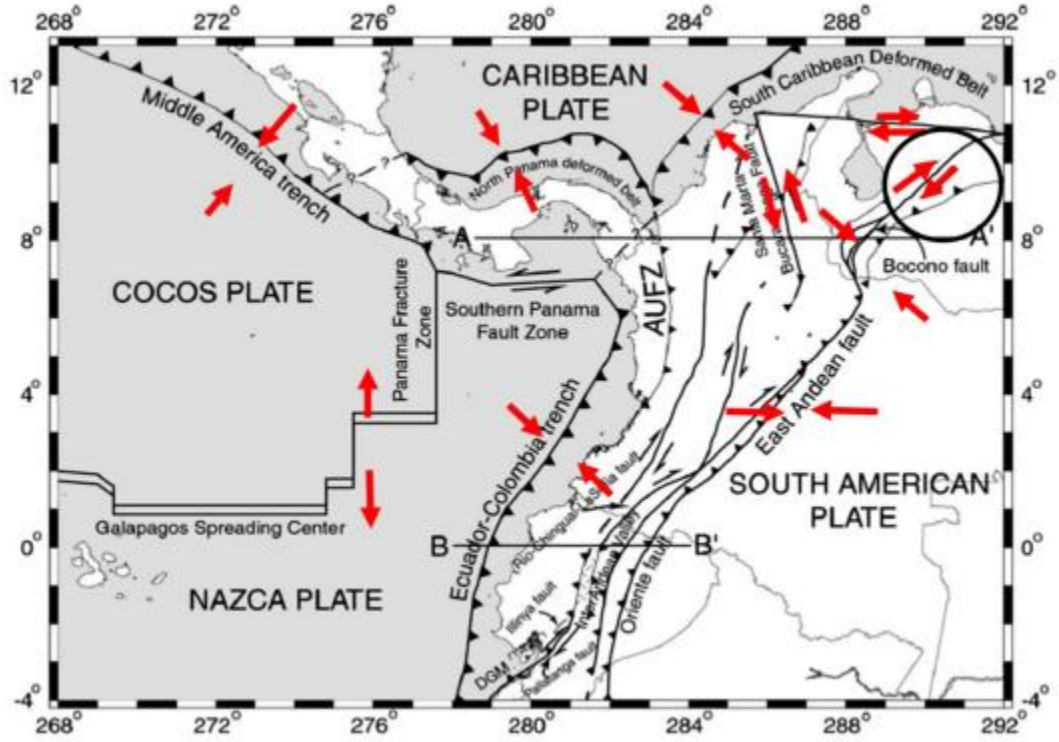

Figure 3: Tectonic plates in the north-western region of South America and Panama. The Yacambú-Quibor project is located in the circled area in the upper right of the figure.
After Trenton et al (2002) with additions by Diederichs (2008).

A limited amount of drilling was done at the tunnel portals but only three vertical boreholes were attempted along the tunnel alignment. The deepest had to be abandoned at 300 m depth because of technical difficulties. Consequently, most of the detailed geology along the tunnel alignment was revealed as the tunnel was excavated and it turned out that, rather than the silicified phyllites anticipated on the basis of the dam site investigations, a high proportion of the rock consists of a highly tectonically deformed graphitic phyllite which behaves in a completely different way than the silicified phyllite. The appearance of the graphitic phyllite at the tunnel face is illustrated in Figure 5.

Figure 4: Downstream face of the ridge in which the Yacambú dam is located. The downstream toe of the concrete-faced rockfill dam can be seen in the centre of the photograph.

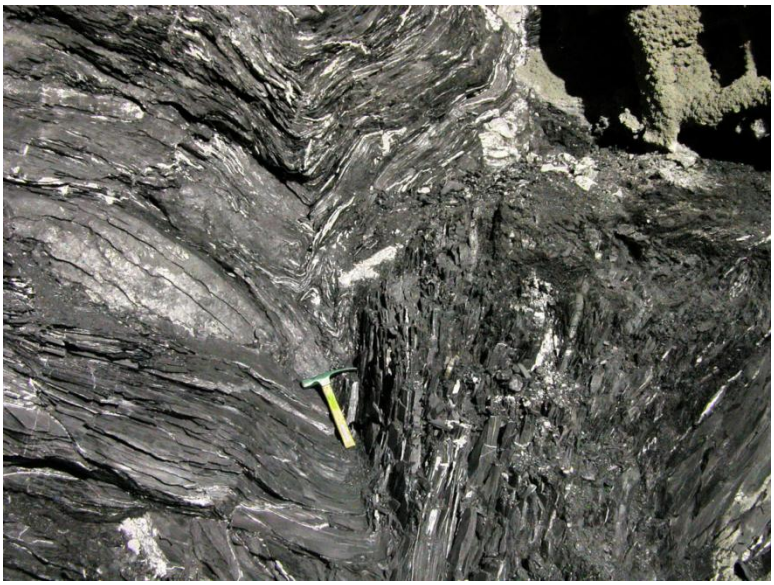

Figure 5: Tectonically deformed graphitic phyllite at the tunnel face.

Construction history

The first contract on the project was awarded in 1975 and work commenced in 1976. Two 4.8 m diameter open face Robbins hard rock Tunnel Boring Machines (TBMs) were mobilised for excavation from the Intake (Entrada) Portal and the Outlet (Salida) Portal. These machines were selected on the assumption that most of the rock that would be encountered would be of reasonable quality and strength, similar to that seen in the silicified phyllites at the dam site. An inclined access adit, with a portal located about 6 km from the Outlet Portal, was mined by conventional drill and blast methods. The purpose of this adit was to provide early access to the Bocono Fault so that this could be mined manually before the TBM arrived. In later years this inclined adit was utilised for ventilation.

The first contract ended in 1977 at which time the TBMs had progressed 700 m and 1,000 m in the Intake and Outlet drives respectively and 700 m had been mined in the inclined access adit. Slow advance rates of the TBMs were blamed on the single gripper design which was considered unsuitable for the weak foliated rock (Matheson, 2002).

The second contract (1978 to 1979) resulted in the Intake drive being advanced to a total of 1,700 m and the Outlet drive to a total of 1,850 m. In 1979 it became evident that the occurrence of the graphitic phyllite in the tunnel route was a serious problem. According to Dr Siegmund Babendererde (2002), the site manager for the TBM contract, the machine operated very well but significant convergence and floor heave (illustrated in Figure 6) started 50 to 100 m behind the TBM. The ground support system, designed for better rock conditions than those encountered, could not cope with the squeezing conditions. After the TBM had advanced 1,700 m and was operating at a depth of 425 m below surface, the work was suspended during technical and contractual discussions. The TBM in the Outlet drive was removed from the tunnel at this time but the Inlet drive TBM was left in place and it was eventually trapped in the squeezing rock. It was excavated in 1987 during the fourth contract as illustrated in Figure 7.

It is interesting that the inclined adit was advanced conventionally to a total distance of 1,200 m during the second contract and that, in order to deal with squeezing conditions, yielding support was used (Babendererde, 2002). Unfortunately, this European technique for dealing with squeezing conditions was not used in the main drives until the fifth contract (1991 to 1997).

The third contract (1981 to 1984) involved drill and blast excavation in the Outlet drive and the inclined adit which were advanced to total lengths of 4,350 m and 1,900 m respectively. The Intake drive, blocked by the TBM, was not worked on during this contract. The contractual period expired in 1984.

The fourth contract (1984 to 1988) concentrated on the inclined adit and headings. The inclined adit broke through at a total length of 2,000 m and the main tunnel was extended by 1000 m in both directions from the adit headings. The Intake drive TBM was excavated during this contract. The contractual period expired and the project was re-bid.

The fifth contract (1991 – 1997) utilised conventional drill and blast in the Outlet drive and a roadheader in the Intake drive. A total of 4,000 m was added to the Intake drive bringing the total length of this tunnel to 5,700 m. The connection between the drive from the Outlet Portal and the inclined adit heading was broken through and the Outlet drive was extended to a total length of 8,750 m. The contractual period expired and the project was re-bid.

The sixth (1997 to 2002) and seventh (2002 to 2005) and eighth (2005 to 2008) contracts were all carried out by the same Venezuelan contractor using conventional drill and blast methods. Final break-through of the tunnel occurred on 27 July 2008.

Figure 6: Floor heave about 100 m behind the Intake drive TBM in 1979 at a depth of 400 to 425 m below surface.

Figure 7: Excavation of the remains of the TBM in 1987 during the fourth contract.

Geological mapping during construction

During many of the contracts described above, excellent as-built drawings, with longitudinal cross-sections of the geological conditions encountered in the tunnels, were prepared by Sistema HidraulicoYacambú Quibor (SHYQ) geologists. Examples of some of the information contained in these drawings are given in Figures 8 and 9.

At the time of writing (2009) this information is being used to evaluate the adequacy of the as-built tunnel for long term operation as a water transmission tunnel. The rock mass characteristics, the depth below surface, the tunnel profile, the sequence of construction and the installed support are all evaluated to determine whether long term problems can be anticipated and, if so, what remedial actions are required.

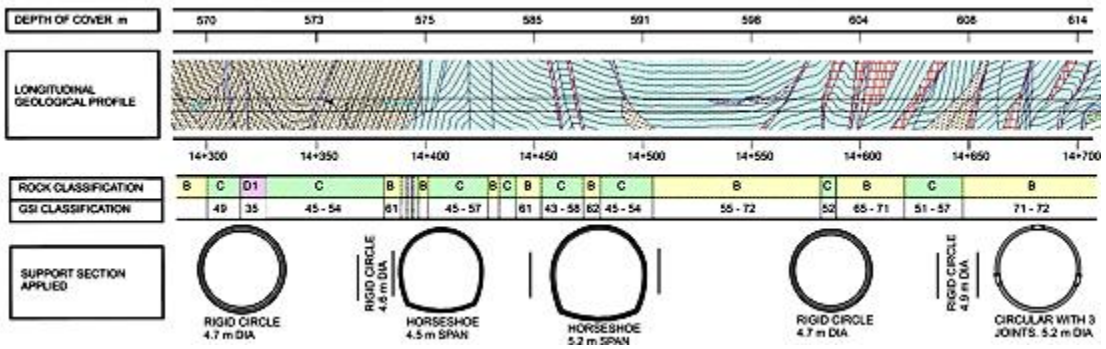

Figure 8: Geological cross-section, rock mass classification and installed support between Chainages 14+300 and 14+700. Information extracted from SHYQ drawings.

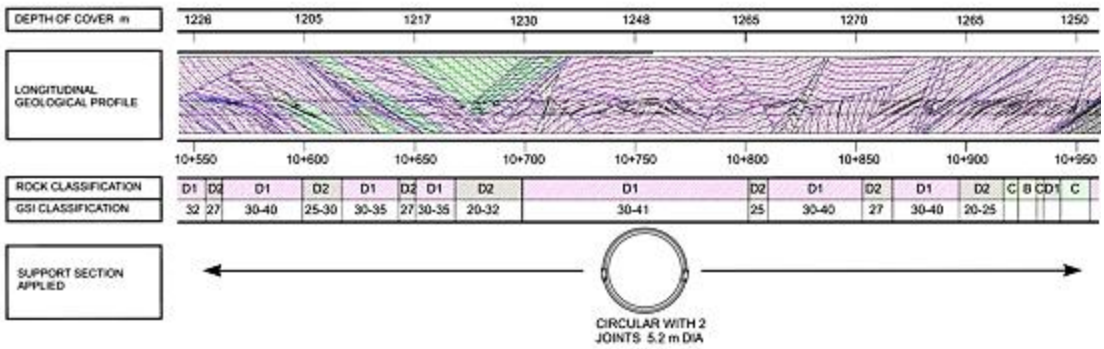

Figure 9: Geological cross-section, rock mass classification and installed support between Chainages 10+550 and 10+950. Information extracted from SHYQ drawings.

Rock mass properties

The 32 years required for the excavation of the Yacambú-Quibor tunnel coincided with significant developments in the field of rock engineering. The tunnel support design methods used in North and South America in the 1970s were based almost entirely on Terzaghi's method of estimating rock loads (Proctor and White, 1946). The rock mass classification systems of Barton et al (1974) and Bieniawski (1974) had only been introduced two years before the start of construction and were virtually unknown in the Americas. Numerical analyses techniques for underground excavation design were in their infancy and personal computers only became available in the early 1980s. European techniques for dealing with squeezing conditions (Rabcewicz, 1963) were seldom used in the Americas and were only used on a regular basis at Yacambú-Quibor from about 1990 onwards.

Descriptive methods for estimating rock mass properties, required for support design calculations, were gradually replaced by rock mass classification methods based on detailed geological observations. Table 1 is an example of one of the early descriptive classifications.

In the mid 1990s the Geological Strength Index (GSI) classification was adopted on site in order to provide information for input into the Hoek-Brown failure criterion (Hoek and Brown, 1997). A GSI classification chart was developed specifically for the phyllites encountered in the Yacambú-Quibor tunnel, based on a model published by Marinos and Hoek (2002) and this chart is reproduced in Figure 10.

A critical component of the rock mass strength determination in the Hoek-Brown failure criterion is the uniaxial compressive strength σ_{ci} of the intact pieces of rock that make up the rock mass. In the case of the graphitic phyllite encountered in the Yacambú-Quibor tunnel, it proved to be difficult to arrive at a consensus on how the strength should be estimated in the field. Most geologists on the project were inclined to assign very low values of 5 to 15 MPa on the basis of the poor appearance of the rock mass and the slickensided nature of the surfaces as illustrated in Figure 11. However, back analyses of the tunnel behaviour suggested that this value should be closer to 50 MPa. Uniaxial compressive tests on oriented specimens of a similar Venezuelan graphitic phyllite by Salcedo (1983) gave the results presented in Figure 12. A maximum UCS of approximately 100 MPa was found for specimens tested normal to schistosity while a minimum of approximately 15 MPa is given for tests on specimens with the schistosity inclined at about 30° to the loading direction. These results are typical for highly schistose rocks and it is not unreasonable to assume an average UCS of 50 MPa for the intact strength of the

individual rock pieces when they are more or less randomly oriented in the rock mass, on the scale of the tunnel, as illustrated in Figure 5.

Table 1: Classification of Yacambú-Quibor rock units.

CLASS	TYPE OF ROCK	CHARACTERISTICS
A	Predominance of silicified phyllite with small amounts of calcareous and/or graphitic phyllite.	Cemented layers from 5 to 10 cm in thickness with high strength and high deformation modulus.
B	Predominance of calcareous silicified phyllite with intervals of graphitic phyllite.	Cemented layers from 2 to 3 cm in thickness with average strength and average deformation modulus.
C	Graphitic phyllite with some intervals of silicified phyllite.	Thin lamination from 0.1 to 1 mm with low strength and highly deformable.
D1	Tectonically deformed, folded and sheared in Classes A, B and C.	Behaves as homogeneous rock mass with zero volume change during deformation
D2	As for D1 with clay gouge in contacts.	Highly plastic deformation with zero volume change

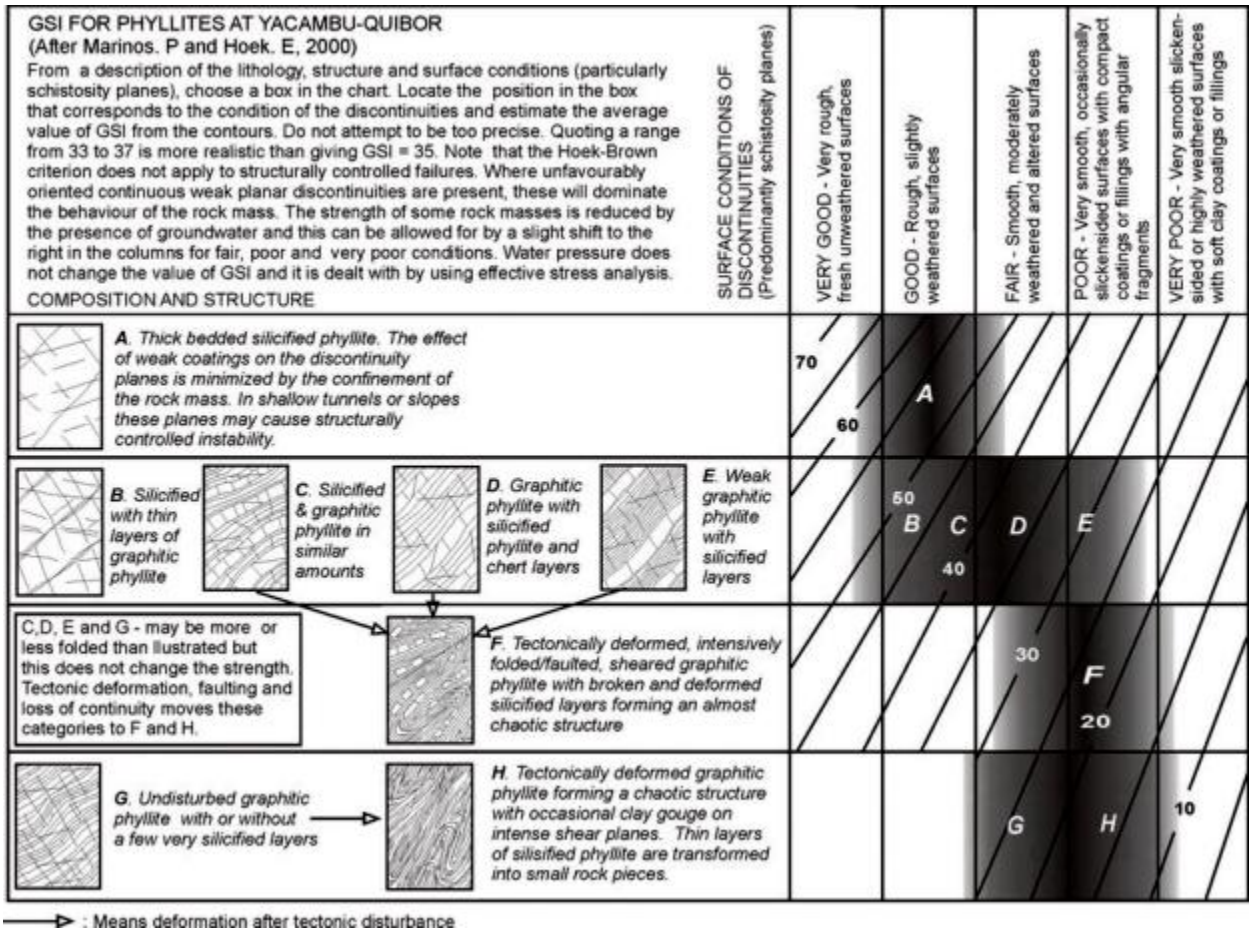

Figure 10: Geological Strength Index (GSI) Chart developed specifically for phyllites in the Yacambú-Quibor tunnel.

Figure 11: Intact sample of graphitic phyllite from Yacambú-Quibor.

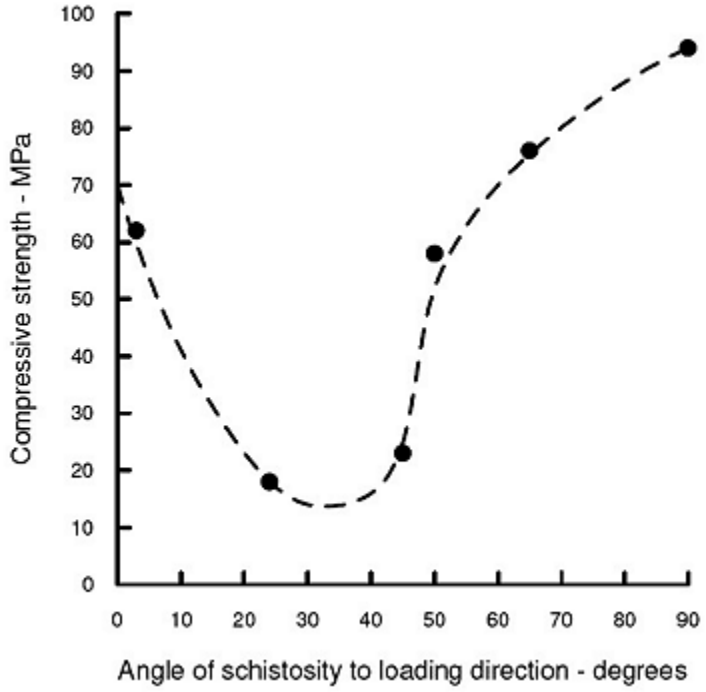

Figure 12: Anisotropic strength of a typical graphitic phyllite.

A third parameter required for the Hoek-Brown criterion is a material constant m_i that is related to the frictional characteristics of the rock material. This constant can be determined by laboratory triaxial tests but, since these tests are seldom carried out for tunnelling projects, the value is typically estimated from a table of typical values (Hoek et al, 2002).

Table 2 gives estimated rock mass characteristics, based on GSI and the Hoek-Brown criterion, for the 5 rock classes described in Table 1. Note that both design values and long term values are listed in this table. The design values are based on short term observations of freshly exposed rock in the tunnel and these values have been used in calculations on the performance of the tunnels during construction. The long term values are based on estimates of the deterioration of the rock mass over time as a result of breakdown of the material and the matrix as a result of creep, progressive breakdown of individual rock pieces under high stress and groundwater percolation. Since some portions of the tunnel were constructed 20 or 30 years ago and some of these have shown signs of distress or have failed during the 32 year construction period, it has been possible to carry out crude checks on the assumed long term parameters by means of back analyses.

Many programs used for the analyses of tunnel behaviour accept input for the Generalised Hoek-Brown failure criterion (Hoek et al, 2002) thereby enabling the user to carry out progressive failure analysis in terms of the non-linear relationships illustrated in Figure 13(a). However, In order to present these analyses in a form that can be understood by readers who are not familiar with the Hoek-Brown criterion, equivalent Mohr-Coulomb strength parameters have been included in Table 2 and plotted in Figure 13(b).

Table 2: Estimated rock mass characteristics based on the Geological Strength Index and the Hoek-Brown failure criterion.

Class	Condition	σ_{ci} MPa	GSI	m_i	m_b	s	a	σ_{cm} MPa	E MPa	c MPa	ϕ deg
A	Design	100	75	10	4.095	0.0622	0.501	32.49	45000	5.76	43.2
	Long term	100	38	10	1.092	0.010	0.513	13.34	7656	2.49	33.0
B	Design	75	65	10	2.865	0.0205	0.502	18.49	26000	3.73	38.6
	Long term	75	32	10	0.882	0.0005	0.520	8.66	3825	1.99	29.0
C	Design	65	50	7	1.174	0.0039	0.506	9.59	11000	2.36	30.3
	Long term	65	25	7	0.481	0.0002	0.531	5.14	2140	1.40	22.9
D1	Design	50	35	7	0.687	0.0007	0.516	5.19	3119	1.59	24.1
	Long term	50	17	7	0.361	0.0001	0.553	2.99	1091	0.99	18.7
D2	Design	50	25	7	0.481	0.0002	0.531	3.95	1646	1.26	21.2
	Long term	50	13	7	0.313	0.0001	0.570	2.51	928	0.84	17.4

Legend:

σ_{ci} - Uniaxial compressive strength of intact rock pieces
GSI - Geological Strength Index
m_i - Material constant m for intact rock pieces
m_b - Material constant m for rock mass
s - Material constant for rock mass
a - Material constant for rock mass
σ_{cm} - Uniaxial compressive strength of rock mass
E - Modulus of deformation
c - Equivalent cohesive strength of rock mass
ϕ - Equivalent friction angle for rock mass

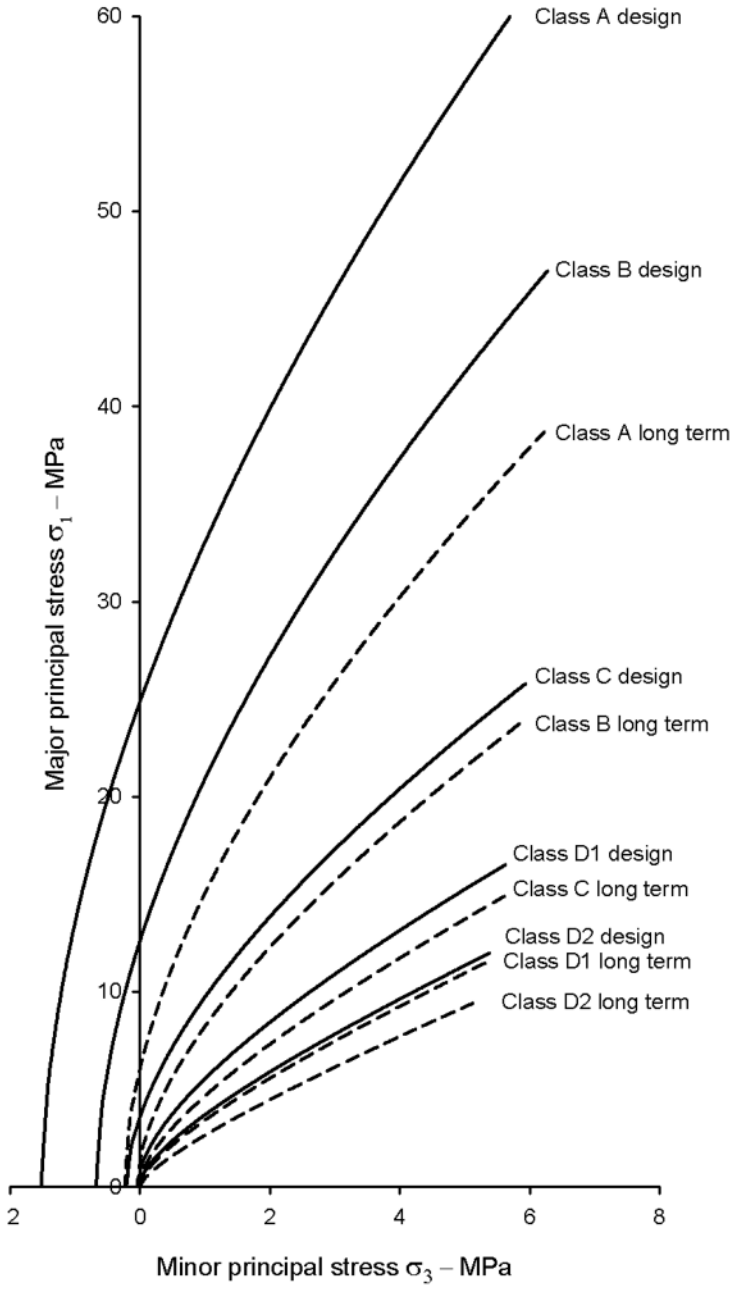

Figure 13: (a) Plot of major versus minor principal stresses for design and long term strength of the 5 rock classes listed in Table 2.

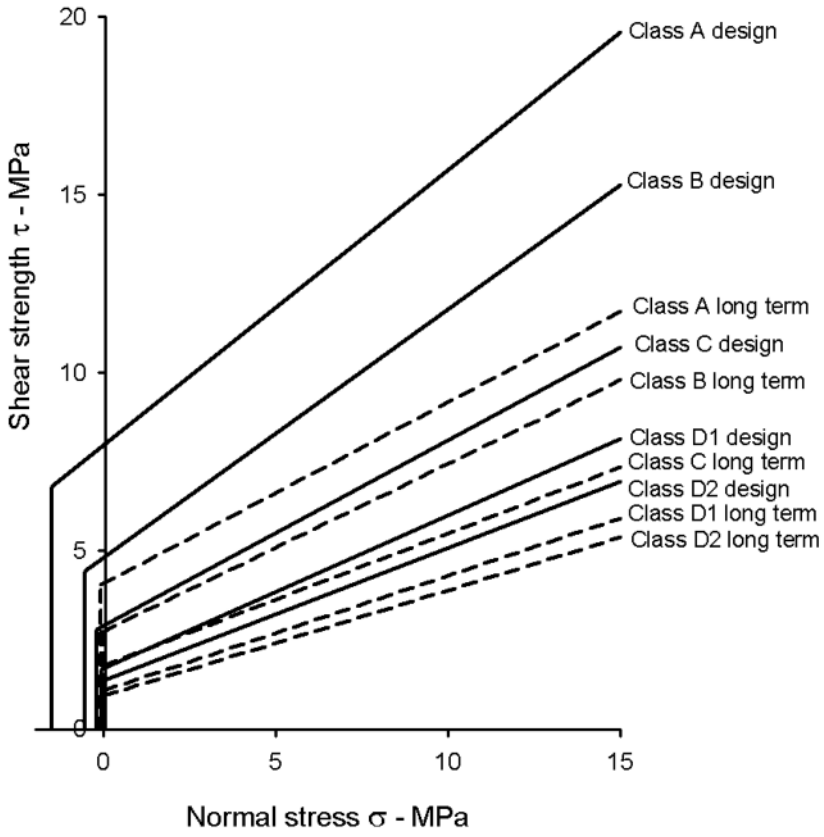

Figure 13 (b) Plot of linear shear strength envelopes (based on equivalent c and ϕ values) for the same rock types.

Potential for squeezing in overstressed rock

As shown in Figure 14, Hoek and Marinos (2000) found that the percentage strain in the rock mass surrounding a tunnel in weak overstressed rock is defined by the equation:

$$\varepsilon = 0.2 \left(\frac{\sigma_{cm}}{p_o}\right)^{-2} \quad (1)$$

where ε is the percentage strain defined by (tunnel closure / tunnel diameter x 100)
σ_{cm} is the uniaxial compressive strength of the rock mass as given in Table 2
p_o is the in situ stress defined by the product of the depth below surface and the unit weight of the rock mass.

The ratio of plastic zone diameter d_p to tunnel diameter d_p is given by the equation:

$$\frac{d_p}{d_o} = 1.25 \, \frac{\sigma_{cm}}{p_o}^{-0.57} \quad (2)$$

Note that this analysis is based on the assumption that the horizontal and vertical in situ stresses are equal. This assumption is reasonable for very weak rock which cannot sustain high shear stresses such that, over geological time, anisotropic in situ stresses will tend to equalise. This assumption has been confirmed by observations and back analysis of the behaviour of tunnels in highly stressed weak rock masses, including the Yacambú-Quibor tunnel.

Figure 14 gives a plot of equation 1 and it shows that the strain increases exponentially as the ratio σ_{cm}/p_o decreases. Strains of less than 1% are generally of no consequence in tunnels and very light or no support is generally all that is necessary to maintain stability. On the other hand, strains of more than 10% fall into the category of extreme squeezing and it is generally required to use yielding support in order to accommodate these large deformations. The design of yielding support systems is discussed in the next section of this paper.

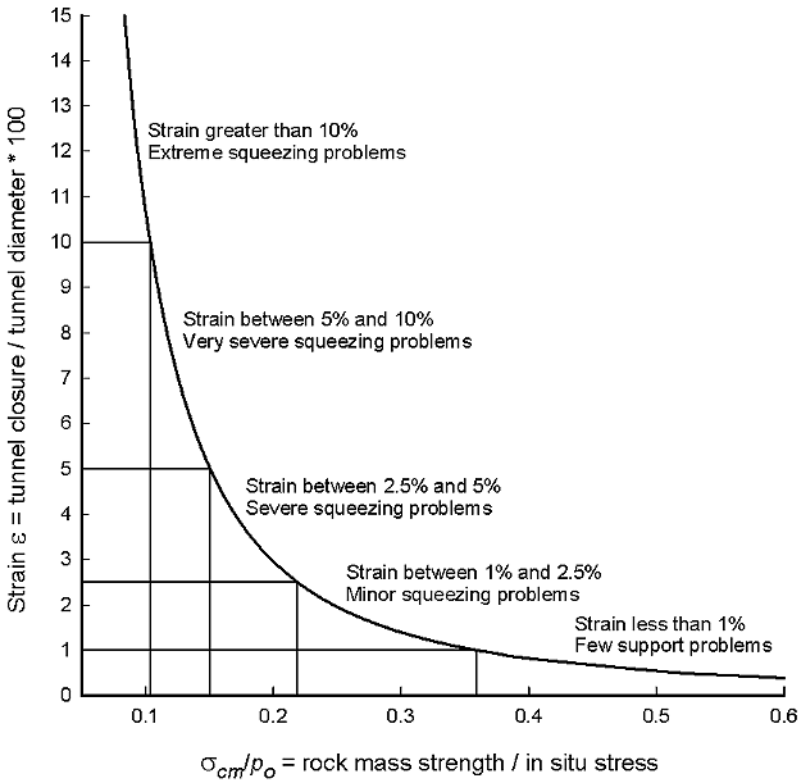

Figure 14: Approximate relationship between strain and the degree of difficulty associated with tunnelling through squeezing rock. Note that this curve is for tunnels with no support.

Based on equations 1 and 2, Figure 15 presents plots of percentage strain and the ratio of plastic zone to tunnel diameter along the Yacambú-Quibor tunnel, assuming that the tunnel is unsupported. It can be seen that, under the highest cover, there are significant lengths of the tunnel that have been assessed with strains in excess of 10% and plastic zone diameters of more than 3 times the tunnel diameter. These estimates are for the short term rock mass properties and apply to the behaviour of the tunnel during and shortly after construction

In the analysis carried out by the authors, the long term behaviour of the tunnel is estimated by assigning the long term rock mass properties (Table 2) to the material contained within the plastic zone. This requires a numerical analysis for each case since there are no analytical solutions currently available for

this problem. It has been found that, for percentage strains in excess of 10% and plastic zone diameters of more than 3 times the tunnel diameter, the long term strain can increase to 20 or 30% which represents extremely severe squeezing.

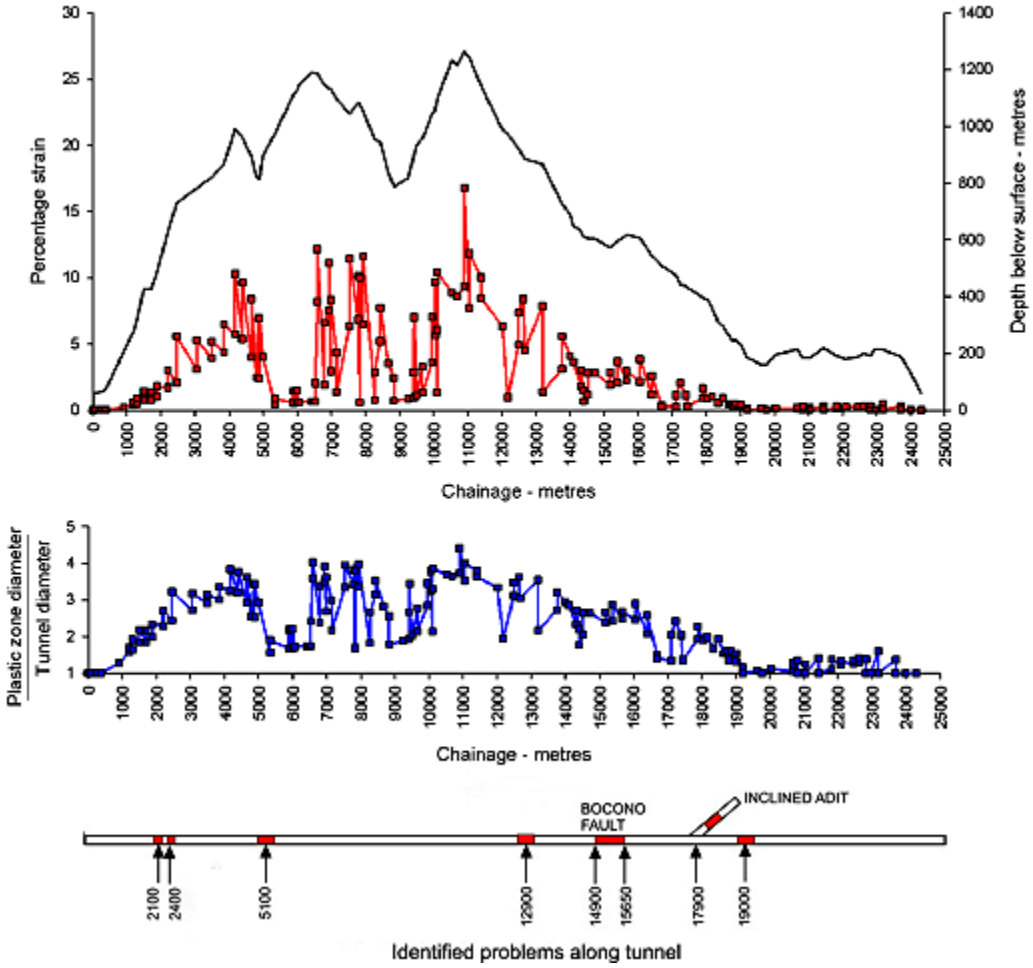

Figure 15: Percentage strain, plastic zone size and identified problems along the tunnel.

Most of the identified problems in the lined tunnel, shown at the bottom of Figure 15, are associated with significant strains and plastic zone diameters. However, other areas with even higher strains have not exhibited problems. This suggests that the success of the tunnelling operation is heavily dependent upon the design of the lining. This conclusion is confirmed by analysis of the construction history of the tunnel which shows that problems occurred where inappropriate lining designs were applied or where the incorrect sequence of support and lining installation was used.

Design of support and final lining

When a tunnel is mined into a rock mass in which the stresses are high enough to induce failure, a zone of failed rock is formed around the tunnel. This zone, frequently referred to as the "plastic zone" is illustrated in the sections given in Figure 16 a and b.

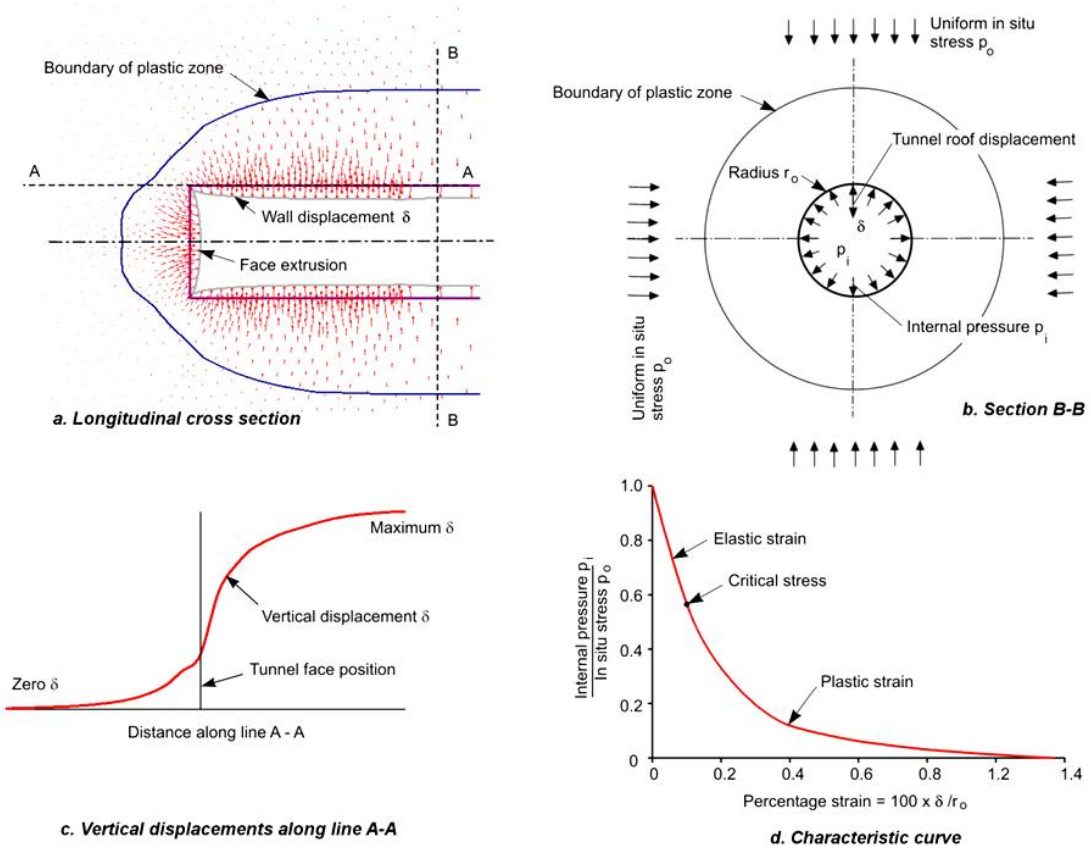

Figure 16: Development of a plastic zone and associated displacements as a tunnel advances through overstressed weak rock

In constructing this figure it is assumed that the tunnel is circular, the horizontal and vertical in situ stresses are equal and an internal pressure p_i acts inside the tunnel. It is also assumed that the response of the rock mass is instantaneous, i.e. time dependent behaviour of the rock mass surrounding the tunnel is not taken into consideration. This could be considered a serious deficiency in the analysis since practical observations of tunnelling in highly stressed ground confirm that there is almost always a strong time-dependency to the rock mass behaviour.

The time-dependent behaviour of tunnels has been discussed extensively in geotechnical literature (eg Kaiser et al, 1982) and some authors, notably Wittke (2000) have used rheological models in analysing this behaviour. However, in considering the issues of time-dependency in the Yacambú-Quibor tunnel the authors took the view that estimating the static properties of the rock mass was a difficult enough problem without adding rheological considerations. A pragmatic approach in which the long term strength was reduced to some proportion of the short term strength was therefore adopted. Where possible, back analysis of the tunnel behaviour was used as a basis for calibrating this reduction.

At a distance of say one tunnel diameter in the rock ahead of the tunnel the magnitude of p_i is equal to the in situ stress p_o. As the tunnel advances the magnitude of p_i reduces. Because of the three-dimensional stress distribution in the rock surrounding the face, the pressure p_i only falls to zero about one tunnel diameter behind the face.

The size of the plastic zone and the magnitude of the displacements in the rock mass surrounding the tunnel increase as the internal support pressure p_i decreases. Figure 16c shows the vertical displacements measured along the line A - A in the roof of the tunnel and this plot is generally known as the Longitudinal Displacement Profile. Figure 16d shows the convergence of the tunnel, expressed as a percentage strain, against the ratio p_i/p_o and this curve is generally known as the Characteristic Curve for the tunnel.

The Longitudinal Displacement Profile depends upon the properties of the rock mass and the in situ stresses which, in turn, define the size of the plastic zone. Figure 17 shows the variation in the shape of this profile for different ratios of plastic zone to tunnel diameters (Vlachopoulos and Diederichs, 2009). These curves are important for determining the displacements at the tunnel face and at the time of support installation.

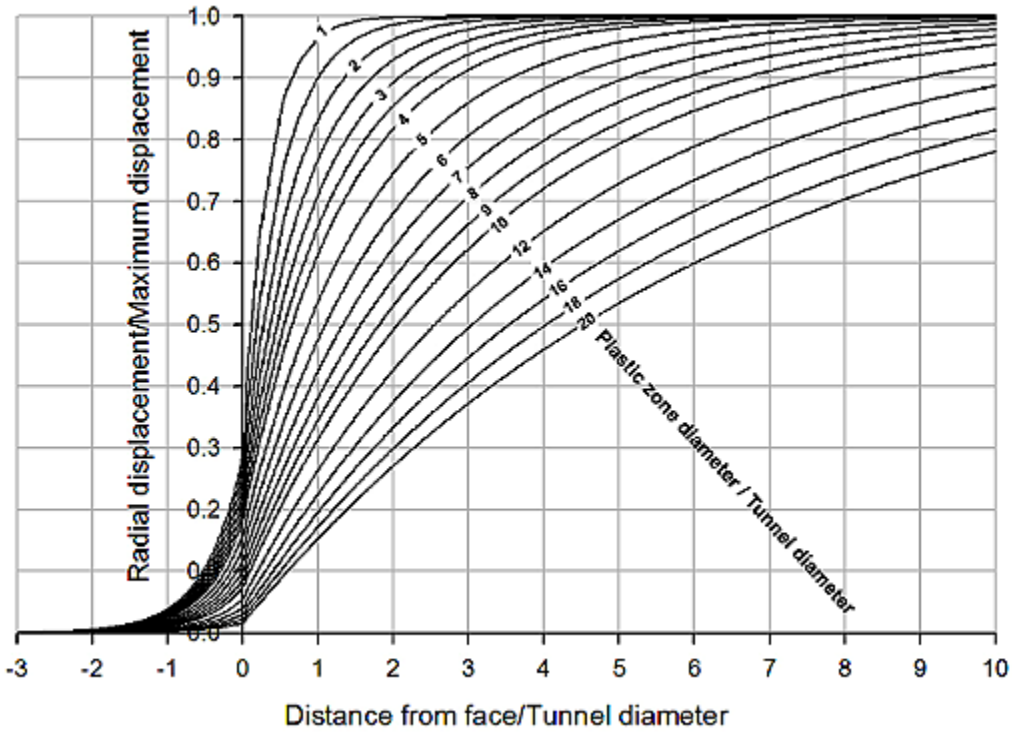

Figure 17: Longitudinal Displacement Profiles for different ratios of plastic zone to tunnel diameter.

Consider the practical example of a 5.2 m diameter section of the Yacambú-Quibor tunnel mined at a depth of 1000 m below surface in class D2 rock. A finite element analysis, using the Rocscience program Phase2 Version 7, was carried out to determine the size of the plastic zone and the tunnel convergence for an unsupported tunnel. The input parameters used in this analysis are listed below.

Depth below surface	1000 m
Unit weight of rock mass	0.026 MN/m^3
In situ stress	26 MPa
Design cohesive strength c	1.26 MPa
Design angle of friction □	21.2 degrees
Design Deformation Modulus E	1646 MPa
Long term cohesive strength c	0.84 MPa
Long term angle of friction □	17.4 degrees
Long term deformation modulus E	928 MPa

Characteristic curves for both design and long term conditions are plotted in Figure 18. Note that, in calculating the characteristic curve for the long term condition, the long term rock mass properties have been applied to the plastic zone only since it is assumed that long term changes due to displacement induced damage, air and water circulation and the like will be restricted to this zone.

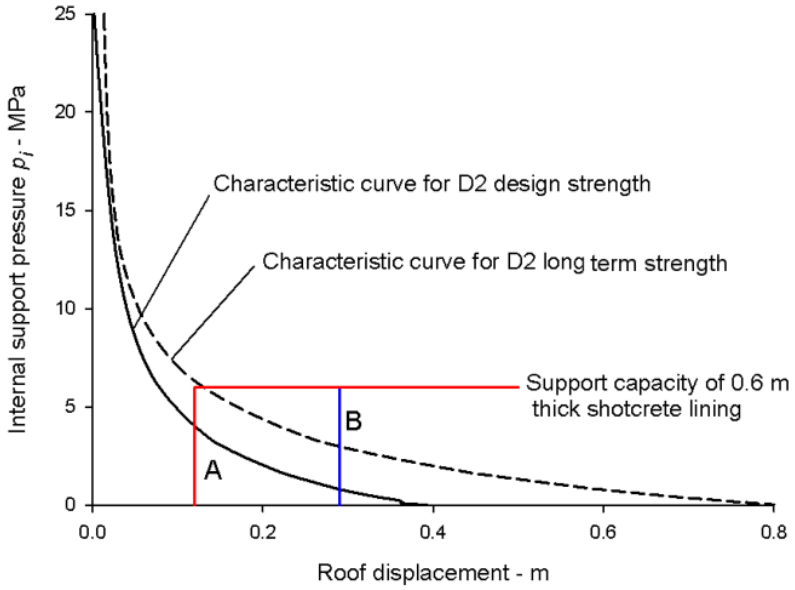

Figure 18: Characteristic curves for an unsupported tunnel in D2 rock mass at 1000 m depth.

The radius of the plastic zone for the fully excavated unsupported tunnel for the D2 design strength conditions was found to be approximately 10.4 m. Figure 19 gives a plot of the Longitudinal Displacement Profile for this set of conditions, for a ratio of plastic zone to tunnel radius of 10.4/2.6 = 4. This curve was calculated from the data used in constructing Figure 17, tabulated in Appendix 1.

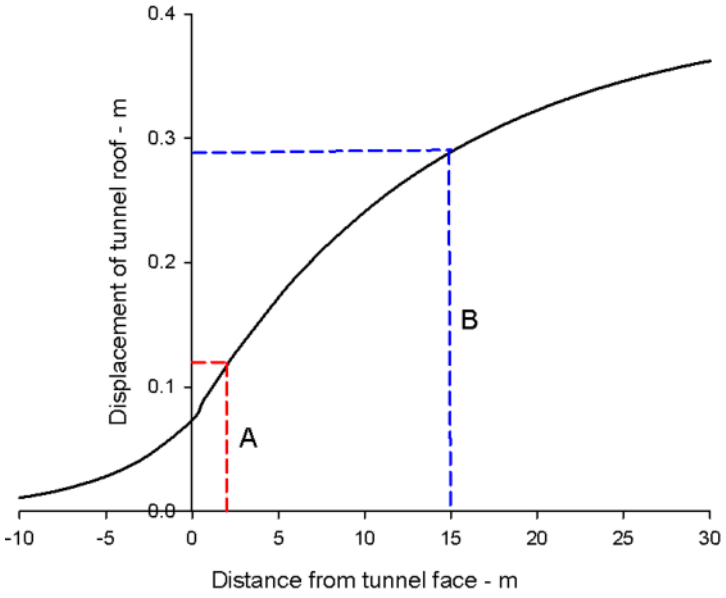

Figure 19: Longitudinal displacement plot for the design conditions in D2 rock.

Based on many years of experience in constructing the Yacambú-Quibor tunnel it was determined that, for the deepest sections of the tunnel in poor quality rock, the tunnel would be circular in shape and that it would be lined with a high quality shotcrete lining. This shotcrete was mixed at surface batching plants adjacent to the portals and transported by rail to the faces where it was applied as a wet mix. Tests on cores taken in situ confirmed that a consistent uniaxial compressive strength of 30 MPa could be relied on for this shotcrete. Since the lining is subjected to predominantly compressive loading, no fibre was added to the lining mix although both steel and polypropylene fibres were used for other special applications.

It was not practical to install and anchor rock bolts in these very weak rock masses and, hence, the only support design decisions were the thickness of the shotcrete lining and the method and timing of installation.

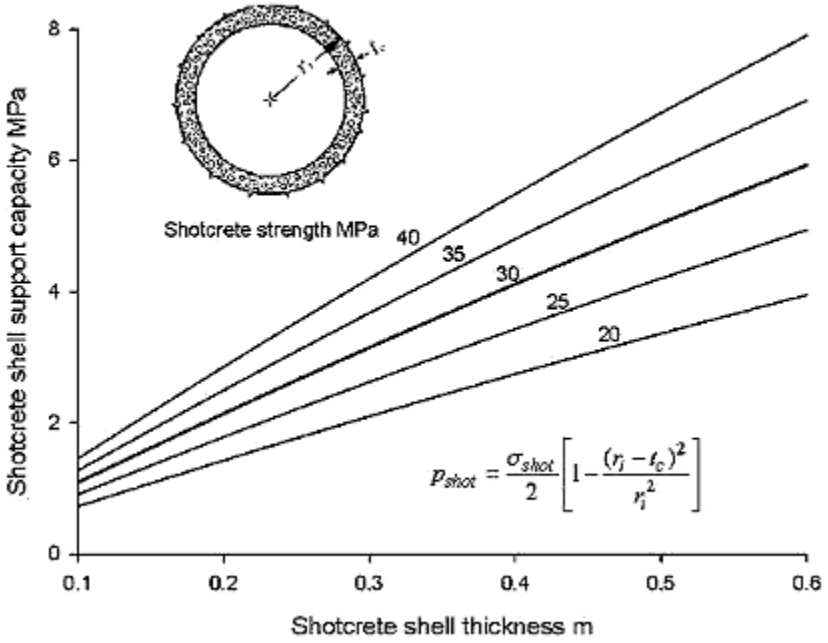

Figure 20: Support capacity of a circular shotcrete lining

Figure 20 shows the capacity of a circular shotcrete lining, assuming equal horizontal and vertical in situ stresses which means that there is no bending in the lining. It can be seen that a 0.6 m thick lining of 30 MPa shotcrete provides a support capacity of approximately 5.5 MPa.

Ideally the lining should be installed as close to the working face as possible in order to provide protection for the workmen. Line A in Figure 19 represents the placement of a 0.6 m lining at a distance of 2 m from the face and the corresponding displacement of the tunnel roof at this time is 0.12 m. This roof displacement is then used to determine the installation point of the lining in Figure 18 in which line A represents the support provided by this lining, assuming that it is infinitely stiff.

Line A in Figure 18 intersects the characteristic line for the design strength at approximately 4 MPa and this represents the support capacity mobilised at the time of installation. Since the capacity of the lining is 5.5 MPa (ignoring the reduced strength of uncured shotcrete for the moment), the factor of safety is given by the ratio of available capacity to mobilised capacity and this is 1.5. However, the available capacity is lower than that required for long term conditions (dashed characteristic curve in Figure 18) and the lining will be overstressed.

An obvious solution to this problem is to delay the installation of the lining and, following the same procedure as used above, lines B in Figures 19 and 18 show the installation of the lining at a distance of 15 m behind the face. In this case the short term (design) factor of safety is approximately 5 while, for the long term conditions, the available lining capacity is approximately twice the required capacity.

Unfortunately it is not practical to install the lining at 15 m behind the face as suggested above since this would result in an unacceptable level of risk to those working in the tunnel. Consequently, if the benefits of delayed lining installation are to be realised, it is necessary to provide some form of safety cage to protect the workers until the shotcrete lining can be fully mobilised. This introduces the concept of yielding support that has been used by miners for many years and, as mentioned earlier, had been employed during the second contract in mining the inclined adit.

Yielding support design

In the case of the Yacambú tunnel several yielding support systems were investigated during the early 1990s and the design finally adopted is illustrated in Figures 21 to 24. The design of this system was based on the requirements that it could be constructed on site from readily available locally manufactured steel sections, it had to be easy to assemble in the limited space available at the tunnel heading and it had to provide sufficient capacity to protect the workmen in the event of a sudden convergence of the tunnel.

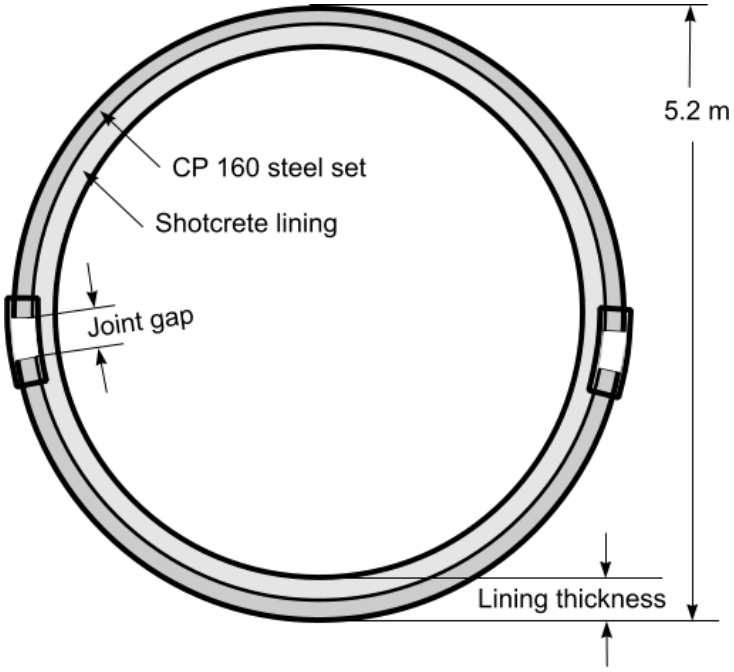

Figure 21: Design details of the yielding support used in the Yacambú-Quibor tunnel.

Figure 22: Details of one of the two sliding joints in the steel sets.

Figure 23: Assembled steel set with two sliding joints in the site workshop.

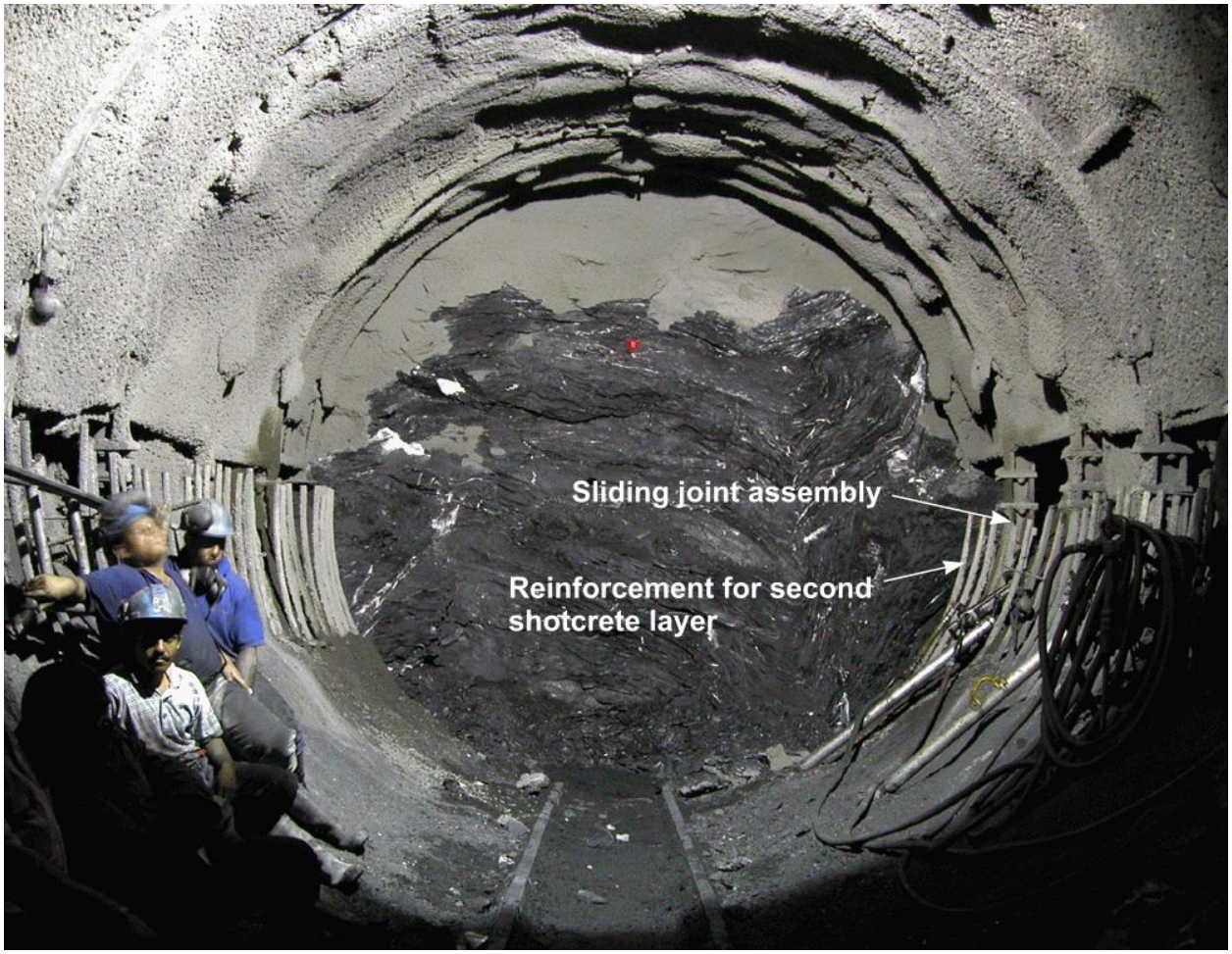

Figure 24: Installation of a circular lining, such as that illustrated in Figure 23, in heavily stressed rock. The sliding joint assembly and the shotcrete window over this gap are shown. Reinforcement for the second layer of shotcrete is visible in this shotcrete gap.

The yielding system illustrated in these figures was installed as close to the face as possible, as shown in Figure 24. In some cases where the stability of the face is a problem, the face was split and a very short top heading driven a distance of 1.5 to 3 m ahead of the following bench. The top half of the steel set was installed in the top heading and the sliding joints and lower half of the arch was installed as soon as the bench was removed. This short bench acted as a face buttress and it proved to be effective in maintain the stability of the face in the worst ground conditions.

Placing of the steel sets, generally at a spacing of 1 m, was followed by the immediate application of a 20 cm thick layer of shotcrete. This was sufficient to embed the 16 cm deep sets and to form a protective shell above the workers. A 1 m wide window was left on both sides of the shotcrete shell to allow the sliding joints to move freely. This window was closed when the sliding gaps had closed or at a distance of about 15 m behind the face, whether or not the gaps had closed. Once the windows had been closed and the initial shell had been fully mobilized, a second inner shotcrete layer of up to 40 cm thick was placed to complete the lining. The appearance of the completed tunnel is shown in Figure 25.

Figure 25: Completed tunnel lining in one of the deepest sections between Chainages 10000 and 12000.

A detailed discussion on the application of numerical analysis to the lining design described above, using the Rocscience program Phase2 Version 7, has been presented by Hoek et al (2008). In the interests of brevity this discussion will not be repeated here but rather these numerical methods will be illustrated by two examples of tunnel failure and the design of rehabilitation measures.

Analysis of failure at Chainage 12750 to 12850

This section of the tunnel was constructed in 2000 as a circular section with a lining illustrated in Figure 26. This lining consisted of WF 6 x 20 steel ribs spaced at 0.8 m with two sliding joints with 30 cm openings, giving a radial convergence of 3.7% strain before locking. These ribs are encased in 40 MPa shotcrete of 0.45 m thickness, reinforced by a layer of 100 x 100 x 7 mm weldmesh (Guevara et al, 2004). The sequence of construction of this lining is not clear in the available documents. It appears that this 0.45 m thick shotcrete may have been placed in a single operation or, at least, the second layer may have been applied after a very short delay.

After about 2 years of service the extensometers registered a sudden increase in deformation as illustrated in Figure 27. This was followed by progressive deterioration and eventual collapse of the lining as illustrated in Figure 28.

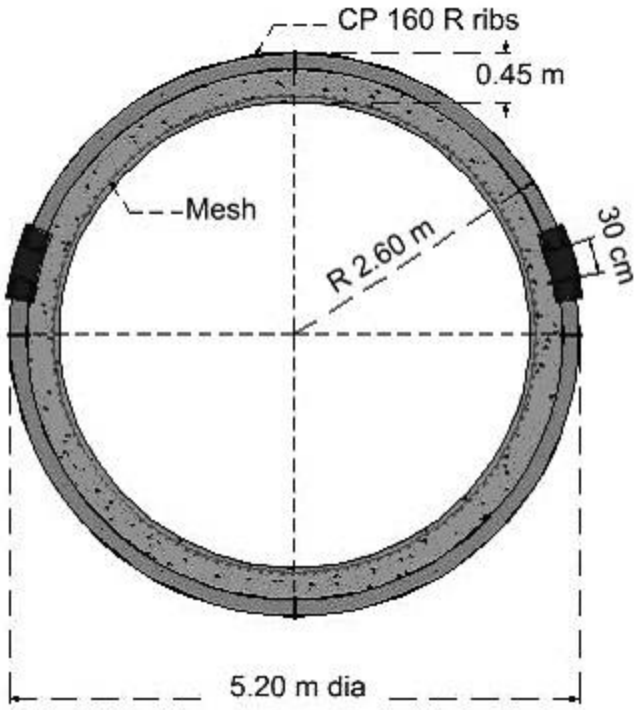

Figure 26: Geometry of the lining used between Chainage 12750 and 12850.

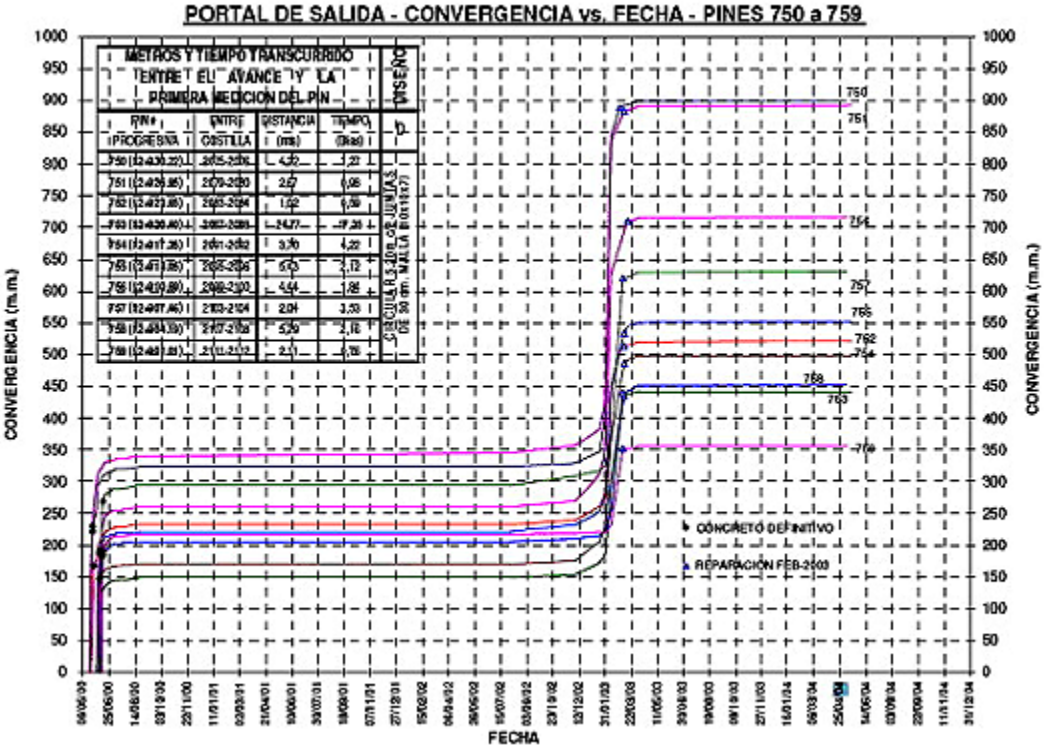

Figure 27: Extensometer measurements in the section between Chainage 12750 and 12850.

Initial damage with cracking of the shotcrete and loss of alignment of the track.

After removal of the cracked shotcrete, significant deformation of the WF 6 X 20 steel ribs could be observed.

In spite of having placed rings of rockbolts to isolate the damaged section, failure propagated to the roof of the section after removal of the damaged shotcrete in the invert.

As the failure developed, with closures of up to 1 m being observed, it was decided to re-mine the tunnel and replace the lining. The photograph shows a repaired section of the tunnel in the foreground and the damaged tunnel in the background.

Figure 28: Evolution of the damage between Chainage 12+750 and 12+850. (Reproduced from Guevara et al, 2004.)

The analysis of this section was based on the following rock mass properties, determined from the information in SHYQ drawing OT-2008-RE-13 and from the paper by Guevara et al (2004).

Parameter	Short term loading	Long term loading
Depth m	855	855
σ_{ci} MPa	50	50
GSI	20	10
m_i	7	7
E MPa	1255	839
c MPa	0.99	0.66
ϕ degrees	20.6	17.0

Since the sequence of lining construction was not known, it was decided to investigate an extreme case in which the steel sets with sliding joints are installed first and then the complete shotcrete lining as a second stage. While this sequence may not represent the actual construction method used, it does simulate a construction "mistake" which can have serious consequences.

The Phase2 model was constructed with a composite lining with the first lining consisting of WF 6x20 ribs, spaced at 0.8 m centers, with 2 sliding joints as illustrated in Figure 26. A yield strength of 350 MPa was assumed for the steel ribs. The second lining consisted of a 0.45 m thick 40 MPa shotcrete shell with 100 x100 x7 mm weldmesh reinforcing. Following the same procedure illustrated in Figures 18 and 19 of the previous section, the first lining was installed at a model stage corresponding to 50% of the maximum convergence of an unsupported tunnel. The second lining was installed after the sliding joints were almost fully closed.

The support capacity curves for the steel ribs are shown in Figure 29. No load is carried at the time of installation since the joints are assumed to slide without resistance. A high axial thrust is induced after closure of the joints and at the end of the construction stage. This short term loading condition results in a factor of safety of approximately 1.2 for the steel ribs.

With the gradual deterioration of the rock mass in the plastic zone surrounding the tunnel, the axial load on the steel ribs increases. For the assumed conditions in which the long term rock mass strength is used and the factor of safety of the steel ribs is reduced to approximately 0.8. Obviously, considering the variability of the rock mass and the loading conditions, failure of some sections of the lining are possible for the conditions illustrated in Figure 28.

The support capacity plots for the shotcrete lining are given in Figure 30. These show that the shotcrete carries very little load under short term conditions and that the factor of safety is approximately 2.2 for long term loading. This is not surprising since the steel ribs carried practically all of the loading before the shotcrete lining was installed. However, failure of the steel ribs under long term loading conditions would result in a transfer of the load carried by the ribs onto the shotcrete lining and this would almost certainly overload the shotcrete. In addition, buckling of the steel ribs would cause local spalling of the shotcrete which would reduce its load carrying capacity.

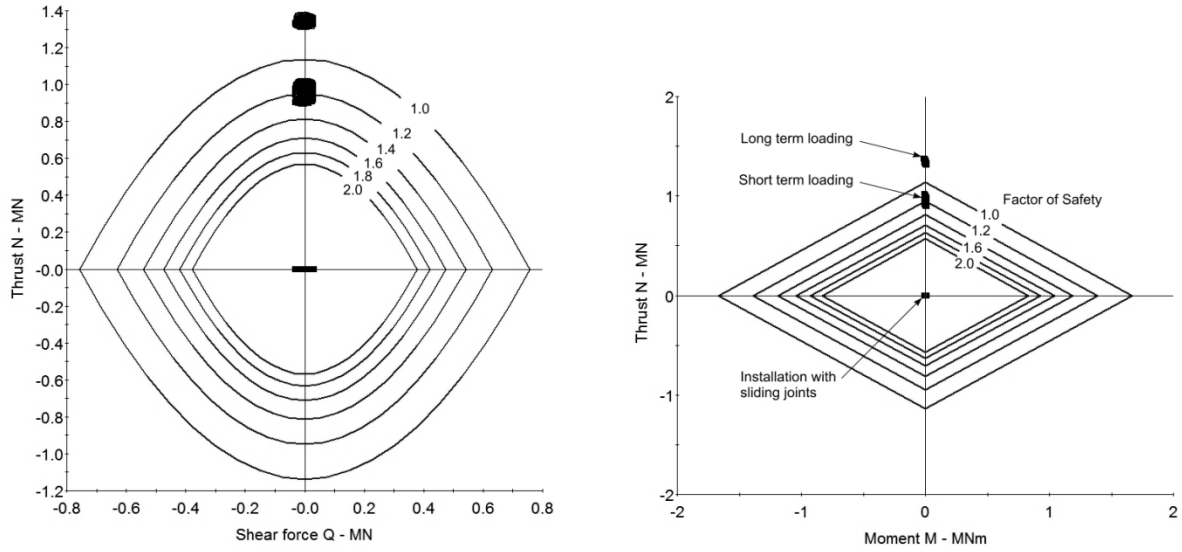

Figure 29: Support capacity plots for steel sets installed without shotcrete.

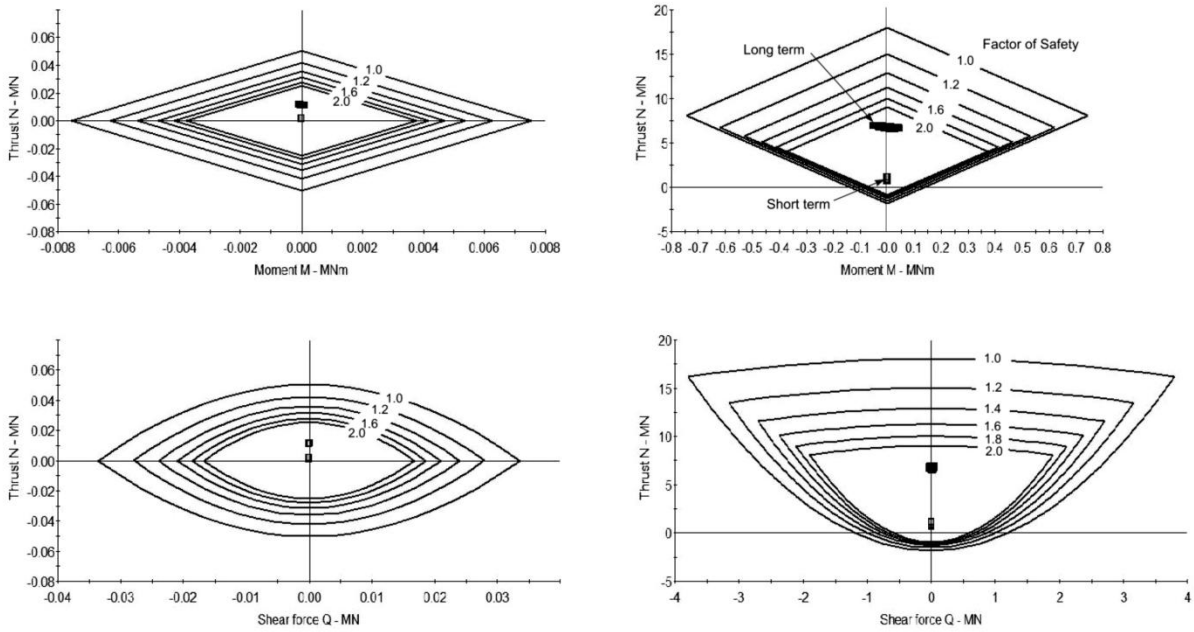

Figure 30: Support capacity 45 cm thick shotcrete lining installed after closure of the sliding joints.

We make no claim that this analysis represents the actual conditions at Chainage 12750 to 12850 but we suggest that it is a very illustrative example. It demonstrates the potential danger associated with incorrect installation sequencing of support elements which, when used correctly, are probably adequate for the loading conditions.

Rehabilitation at Chainage 2100

This section of the tunnel was constructed during fifth contract period (1991 to 1999) with excavation by means of a roadheader of a modified horseshoe shaped tunnel as shown in Figure 31.

An initial 5 cm of shotcrete was placed in order to protect the exposed rock surface and this was followed by W 6 x 20 steel sets placed at 0.8 to 1.3 m spacing. Two sliding joints were included in each set as illustrated in Figure 26. A 20 cm gap in each of these joints allowed a convergence of about 10 cm or 2% before the sets carried load. The sets were embedded in shotcrete with a thickness of 15 to 20 cm. The shotcrete strength was high at approximately 40 MPa. A final layer of 5 to 10 cm of fiber reinforced 40 MPa shotcrete was added to protect the surface.

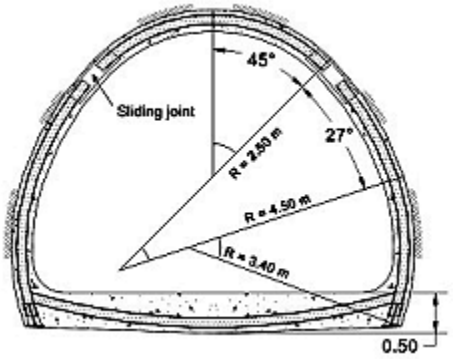

From SHYQ Drawing OT-ER-PE-003

Figure 31: Modified horseshoe section used at Chainage 2100 in type D2 rock with a GSI rating of 26 to 37 at a depth below surface of 570 .

Since the tunnel was excavated by roadheader it was not possible to place the invert at the same time as the steel sets described above. In many cases the invert was not placed until the face had moved ahead approximately 50 m. The invert itself consisted of 50 cm of shotcrete with an embedded invert strut in the form of a W 6 x 20 steel rib.

Failure of the installed support commenced approximately 10 years after construction with progressive deterioration of the invert, followed by overstressing of the steel ribs and shotcrete forming the arch. This failure is illustrated in the photograph reproduced in Figure 32 a. The second photograph (Figure 32 b) shows the final collapse of the tunnel and the rehabilitation work in progress.

a. Damage to invert and arch

b. Rehabilitation of collapsed tunnel

Figure 32: Initiation of failure and final rehabilitation of the tunnel at Chainage 2100.

An analysis of the support capacity of the lining installed in this section was carried out using the Rocscience program Phase2 Version 7 for the following assumed conditions. These conditions were estimated from the information given on SHYQ Drawing number OT-ER-PE-003.

Parameter	Short term loading	Long term loading
Depth m	570	570
σ_{ci} MPa	50	50
GSI	31	15
mi	7	7
E MPa	2388	1045
c MPa	1.04	0.64
ϕ degrees	26.9	21.2

In constructing this model it was assumed that the tunnel invert was placed a long distance (say 50 m) behind the face. This delay in the invert closure means that the arch does not carry any axial thrust but that it is subjected to bending as a result of closure of the tunnel. The support capacity plots in Figure 33 show that the steel carries practically no load while the shotcrete shell is locally overstressed by bending of the lower legs. The short term deformation of the tunnel is complete at this point and, when the invert is installed, it carries no load other then the dead load of equipment in the tunnel.

Plots of the bending moment distribution in the shotcrete lining are given in Figures 34 and 35 for short and long term loading. The high bending moments in the invert shown in Figure 35 are responsible for the initiation of the damage illustrated in Figure 32a.

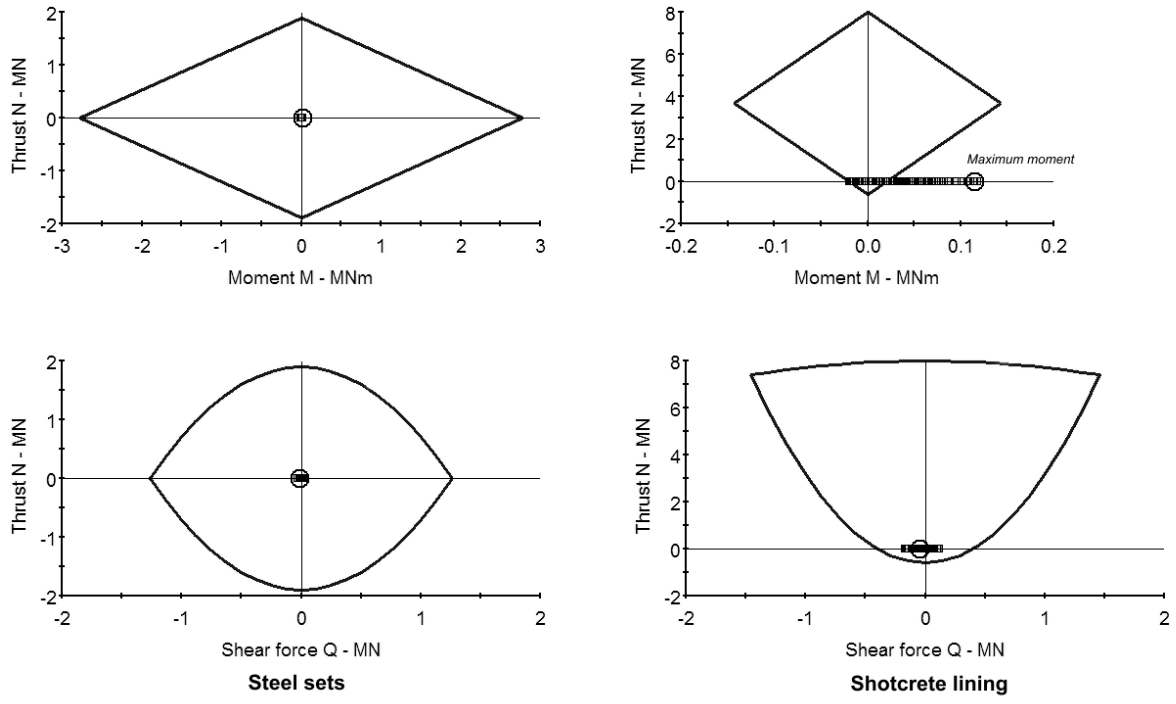

Figure 33: Support capacity plots for the lining with delayed installation of the invert.

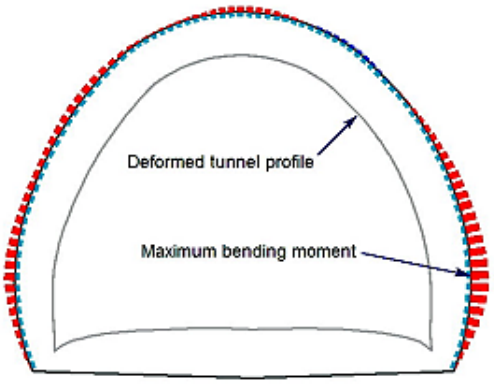

Figure 34: Bending moment distribution in the shotcrete lining for short term loading with the delayed installation of the tunnel invert.

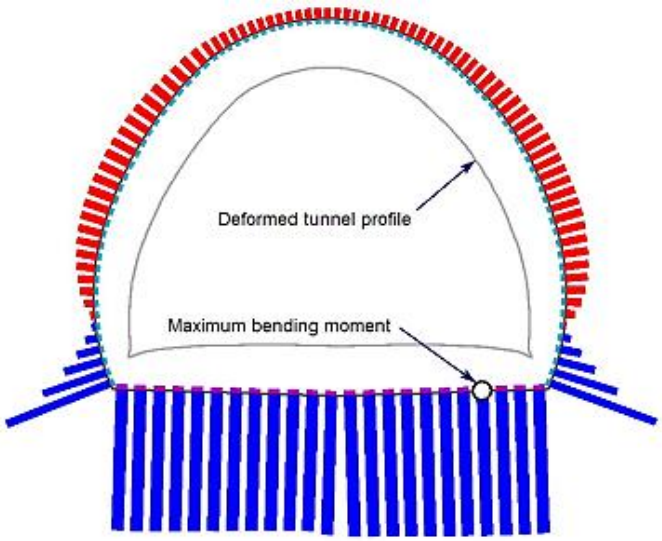

Figure 35: Bending moment distribution in the shotcrete lining for long term loading with the delayed installation of the tunnel invert. The red and blue bars represent moments of opposite sign.

Rehabilitation of the tunnel in this section was carried out by re-mining the collapsed tunnel in sections, as shown in Figure 32b, and installing the lining shown in Figure 36. This lining consists of a 50 cm thick shotcrete shell with reinforcement in the form of two layers of weldmesh. Since a large amount of deformation was associated with failure of the original tunnel, the load carried by the replacement lining is relatively low and there is no need to reanalyse the capacity of this new lining.

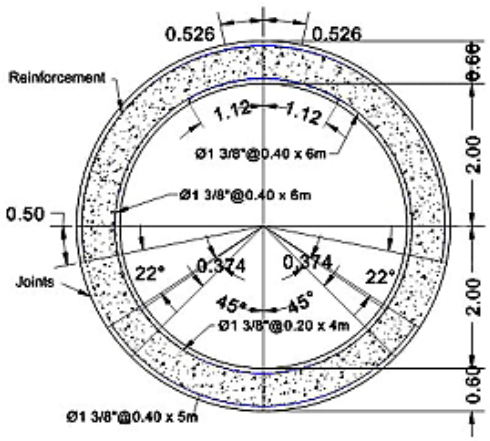

Figure 36: From SHYQ Drawing OT-ER-PE-003

Conclusions

Severe squeezing problems during the construction of the Yacambú-Quibor tunnel presented many challenges to the engineers and contractors on the project. This paper has addressed only those issues related to the design of the support systems. Over the 32 years of construction approximately 30 different support designs were used and, in better rock conditions under moderate stress conditions, many of these designs were successful. However, in the very weak graphitic phyllites at depths of up to 1200 m below surface, squeezing could only be handled effectively by installing yielding support in a circular tunnel profile.

Simplified estimates of tunnel support capacity are totally inadequate under these conditions since by far the most important factor to be taken into account in the design of support is the sequence of installation and activation of the different support elements. While it is necessary to provide support immediately behind the face in order to protect miners in the tunnel, the capacity of this support cannot be activated immediately otherwise the lining will be overstressed. Delaying the activation requires a system that is robust enough to provide emergency support in the event of a tunnel collapse close to the face but is flexible enough to delay the support activation for as much as 3 tunnel diameters behind the face. The use of simple sliding joints in steel sets proved to be a very effective means of achieving both of these goals.

Two case histories have been presented to illustrate different mechanisms that can lead to failure of the support system, even if sliding joints are present. These mechanisms are related to the sequence of installation of the different support components. Fortunately, because squeezing tends to be a slow and gradual process, the failure of the tunnel can be managed by appropriate remedial measures. Although highly undesirable from a cost and schedule point of view, re-mining and reconstruction of the support tends to be relatively simple since the failure of the original lining has also served to relieve the stress concentrations in the rock mass surrounding the tunnel.

Acknowledgements

Permission from Sistema Hidráulico Yacambú-Quibor C.A. to publish this paper is acknowledged.

The authors have been involved in this project for 18 and 26 years respectively and, during this time, have worked with many outstanding engineers and geologists in SHYQ, the contractors and several consultants. It is not possible to list all of these individuals but we thank them for their involvement and the valuable contributions that they have made.

References

Babendererde, S. (20002). Personal communication

Barton, N.R., Lien, R. and Lunde, J. 1974. Engineering classification of rock masses for the design of tunnel support. Rock Mech. 6(4), 189-239.

Bieniawski, Z.T. 1973. Engineering classification of jointed rock masses. Trans S. Afr. Inst. Civ. Engrs 15, 335-344

Diederichs, M.S. (2008). Personal Communication..

Hoek, E, Carranza-Torres, C.T, Corkum B. Hoek-Brown failure criterion-2002 edition. 2002. In Proceedings of the Fifth North American Rock Mechanics Symp., Toronto, Canada, 1: 267–73. (http://www.rocscience.com/hoek/references/H2002.pdf)

Guevara, R., Cerda, P. and Carrero, R. 2004. Túnel Yacambú-Quibor, Experiencia de Construcción - Reparación Tramo entre las Progresivas 12+800 a 12+950. XVIII Seminario Venezolano de Geotécnia Geoinfraestructura: "La Geodesia en el Desarrollo Nacional".

Hoek, E. and Brown, E.T. 1997. Practical estimates or rock mass strength. Intnl. J. Rock Mech. & Mining Sci. & Geomechanics Abstracts. 34 (8), 1165-1186. (http://www.rocscience.com/hoek/references/H1997.pdf)

Hoek, E, Marinos, P and Benissi, M. 1998. Applicability of the Geological Strength Index (GSI) classification for very weak and sheared rock masses. The case of the Athens Schist Formation. Bull. Engg. Geol. Env. 57(2), 151-160.

Hoek, E. and Marinos, P. 2000. Predicting Tunnel Squeezing. Tunnels and Tunnelling International. Part 1 – November 2000, Part 2 – December, 2000. (http://www.rocscience.com/hoek/references/H1998d.pdf

Hoek, E, Carranza-Torres, C.T, Diederichs, M.S. and Corkum, B. 2008. Integration of geotechnical and structural design in tunnelling. Proceedings University of Minnesota 56th Annual Geotechnical Engineering Conference1. Minneapolis, 29 February 2008, 1-53. (http://www.rocscience.com/hoek/references/H2008.pdf)

Kaiser, P.K., Maloney, S. and Morgenstern, N.R. 1982. Time-dependent behaviour of tunnels in highly stressed rock. Proc. 5th ISRM Congress of Rock Mechanics. Australia. D329-336.

Marinos, P and Hoek, E. 2000 GSI – A geologically friendly tool for rock mass strength estimation. Proc. GeoEng2000 Conference, Melbourne. 1422-1442. (http://www.rocscience.com/hoek/references/H2000a.pdf)

Matheson, B (2002). Concrete know-how in Venezuela. Tunnels and Tunnelling International, July 2002.

Proctor, R.V. and White, T.L. (1946). Rock tunnelling with steel supports. Youngston, Ohio: Commercial Shearing and Stamping Co.

Rabcewicz, L.V. (1964) The New Austrian Tunneling Method, Water Power, Part I, November 1964; Part II, December 1964, 511-515; Part III, January 1965, 19-24.

Sánchez Fernándes, J.L., and Terán Benítez, C.E. (1994). "Túnel de Trasvase Yacambú-Quibor. Avance actual de los trabajos de excavación mediante la utilización de soportes flexibles aplicados a rocas con grandes deformaciones". Integral approach to applied rock mechanics, M. van Sint Jan, ed. Editec, Santiago, 1, 489-497.

Salcedo D.A. Macizos Rocosos: Caracterización, Resistencia al Corte y Mecanismos de Rotura. Proc. 25 Aniversario Conferencia Soc. Venezolana de Mecánica del Suelo e Ingeniería de Fundaciones, Caracas. 143-172 (1983).

Trenkamp, R., Kellogg, J.N., Freymueller, J.T., Mora, H.P. (2002). Wide plate margin deformation, Southern Central America and northwestern South America, CASA GPS observations. J. South Am. Earth Sci. 15, 157–171.

Vlachopoulos, N. and Diederichs, M.S. 2009. Improved linear tunnel displacement profiles for convergence confinement analysis. Submitted to Rock Mechanics and Rock Engineering.

Wittke, W. 2000 Stability analysis for tunnels. Verlag Glückauf GmbH: Essen